Path Planning and Fiber Angle Optimization of Continuous Fiber Composites for Additive Manufacturing

Mariana Manuel Martins Fernandes
mariana.m.fernandes@tecnico.ulisboa.pt

Instituto Superior Técnico, Universidade de Lisboa, Portugal

December 2019

Abstract

Since its early days, the aerospace industry has aimed to improve aircraft performance and efficiency. Economic, energetic and, most recently, environmental issues have become critical design drivers. Therefore, lighter and stiffer materials, which lead to less fuel consumption, are one of the most important research topics in the industry.

In this line of thought, Additive Manufacturing (AM) technologies have been successfully implemented in a series of applications. Fused Deposition Modeling (FDM), one of the most popular AM techniques, is a method for fabricating thermoplastic parts, used as rapid prototyping with advantages of low cost, minimal waste and ease of material change. Due to the intrinsically limited mechanical properties, the idea of adding reinforced materials (such as carbon fibers) into plastic materials to form thermoplastic matrix carbon fiber reinforced plastic (CFRP) composites emerges.

Furthermore, the recent developments in AM technologies lead to the emergence of new design techniques which go beyond the classical design rules, thus leading the designer to find innovative and more efficient solutions like the variable angle-tow (VAT) composites. VAT composites allow taking advantage from the benefits related to the curvilinear fibre path in the most effective way, though their utilisation unavoidably implies an increased complexity of the design process.

The main goal of this thesis is to implement a path planning algorithm and optimize both the printing time and the stiffness of the produced part, making use of the MATLAB Genetic Algorithm, for curved and straight fibers.
Keywords: Additive Manufacturing, Fused Deposition Modeling, Carbon Fiber Reinforced Plastic, Variable Angle-Tow Composites, Path Planning, Genetic Algorithm.

1. Introduction

Additive Manufacturing processes allow a higher degree of freedom when compared to traditional manufacturing methods. This technology enables the production of complex surfaces and internal structures that can translate into parts that present greater structural loads at lower masses. These properties are particularly interesting for the aerospace industry, since the smallest mass reduction can yield a significant fuel cost reduction over the lifetime of a vehicle [1]. Laminated parts built using Fused Deposition Modelling (FDM) are becoming increasingly popular. However, these parts, normally made of thermoplastic polymers, lack strength and stiffness, restricting their application. Therefore, there is a critical need to improve the strength of FDM-fabricated pure thermoplastic parts to overcome these limitations. One of the possible methods is adding reinforced materials into plastic materials to form thermoplastic matrix carbon fiber reinforced plastic (CFRP) composites [2]. However, in order to produce composite parts by FDM with specific characteristics, it is essential to achieve models for the material mechanical properties. The main goal of the additive manufacturing industry is to be side by side the traditional industry, and in a fast and continuously changing world, the speed of the processes is of great importance. Considering this, another important variable to be considered is the printing time.

Optimization with Genetic Algorithm (GA) provides a way to bypass much of manual iteration. In order to navigate a vast and dynamic design space, the dynamics of biological evolution suggest ways of continuously expanding the design space towards new and unexplored possibilities [3]. The Genetic Algorithm Optimization is able to take the boundary conditions, loading, performance targets and objectives as inputs, and output an optimal structure for whichever chosen object. GA has been used in several researches for composite optimization in recent years, and it has been revealed as a good optimizer in this field [4][5][7]. To the best knowledge of the author, there is no study for the integration of the structural optimization with the path planning of continuous fiber reinforced composite structures. The objective of this work is the development of an optimization framework for the continuous Fibre-reinforced composite structures to maximize the structural performance and minimize printing time with the minimum number of cuts during the placement (for both straight and curved fibers), using additive manufacturing. Even though composites have been around for a while now, emerging AM techniques like automated fiber placement (AFP) or the continuous tow shearing (CTS), allow to go further from the traditional design rules, leading the design away from the classical straight fibers format.

2. Background

2.1. Outline of the Optimization Process

The outline of the work is presented in this section. A flowchart presented in Figure 1 represents an overview of this thesis work in terms of activities. The different colors in the flowchart were introduced in order to differentiate the software where the actions take place: the first two blocks actions are performed in MATLAB, while the last block action is performed in Abaqus.

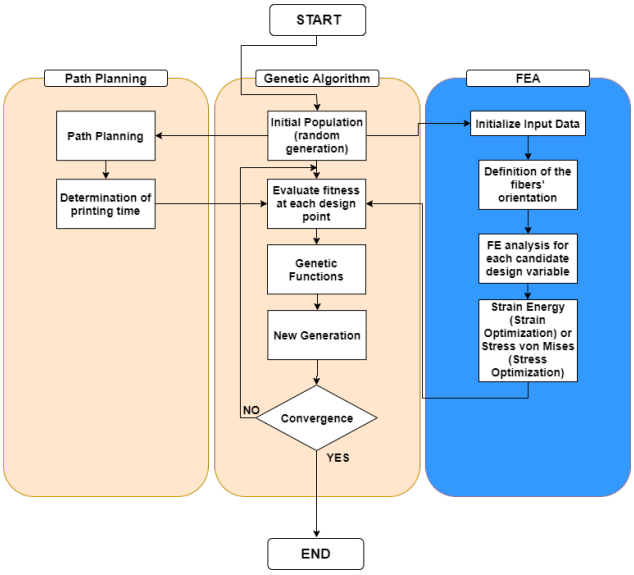

Figure 1: Flowchart

The whole process of optimization starts with the assignment of a random population, which will lead to the initial design. This initial design is plotted using a MATLAB code which is based in a path planning algorithm. From this initial design, two different variables are obtained: **Printing Time** - Obtained from the MATLAB code mentioned above; **Strain Energy or Stress Von Mises** - Obtained from the Finite Element Analysis.

Having computed both variables, the optimization is ready to run and the whole process is repeated until the convergence criteria is achieved.

2.2. Software selection

To develop the finite element analysis, firstly, a suitable FE simulation software must be selected. For this work, Abaqus 6.14.1, from the Dassault systems suite, is chosen. This particular FE software is widely used in the aerospace composites industries due to it reliable and versatile simulation capabilities.

2.3. Pre-Processing: Python Scripts

Several tasks in Abaqus are time consuming and practically impossible to perform in GUI (Abaqus/CAE). To perform a repetitive task or vary parameters of a simulation as part of an optimization study, it can only be done through Python Scripts [6]. An added advantage to scripting is that the entire analysis is saved in a small readable text file. The flowchart presented in Figure 2 represents the pre-processing in detail along with the flow of the python script.

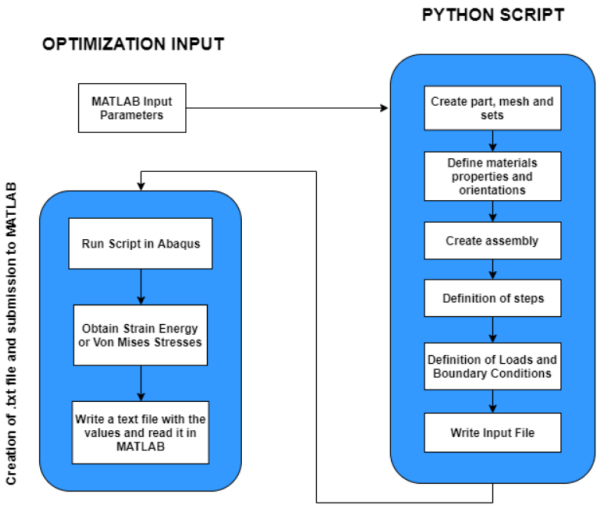

Figure 2: Activities of the pre-processing

2.4. Mechanical Properties of 3D Printed Carbon Fiber Composites

With the ultimate goal of getting results as accurate as possible, the values of layer thickness used in this study are from the The Mark Two [8]. This printer has the capability of printing parts in both concentric and isotropic fill types. Regarding the elastic properties of Nylon, they were computed in a study by Melenka et al [9].

The typical carbon fiber yarn properties were acquired from [10].

It is important to mention that the carbon fiber yarn density considered was of 28%. Having this, the conditions are gathered to compute the final properties of the 3D printed material:

Symbol	Units	Value
E_{11}	Pa	18.66×10^9
E_{22}	Pa	1.535×10^9
G_{12}	Pa	0.5863×10^9
E_{23}	Pa	0.5730×10^9
ν_{12}	-	0.336
ν_{23}	-	0.340

Table 1: Properties of the material

2.5. Functional Fiber Path Representation

Tatting and Gördal generalized the path definition formulation to vary linearly along and arbitrary axis x', where $\theta(x')$ is defined as:

$$\theta(x') = \phi + (T_1 - T_0)\frac{|x'|}{d} + T_0 \tag{1}$$

and T_0 and T_1 are the fiber angles at the beginning and at the end of the characteristic length d. Regarding ϕ, it represents the inclination of x' with respect to the global x-axis. Figure 3 is presented next in order to clarify the stated idea:

In order to obtain the equation to implement the fibers in MATLAB, the integral of equation 1 has to be computed, and the final equation is represented in 2:

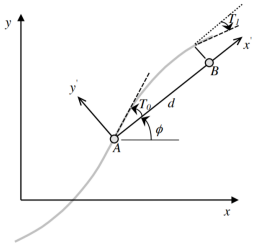

Figure 3: Curved Fiber

$$y'(x') = \phi x' + (T_1 - T_0)\frac{|x'|}{2d}x' + T_0 x' \tag{2}$$

3. Implementation

3.1. Material Definition for Curved Fibers

In order to define the material in the FE software for curved fibers, the properties were computed according to the angle of rotation θ of each element and assign them to the element; In order to make use of equation 1, it is necessary to determine the coordinates of the center of the elements. However, Abaqus does not have a function that allows one to determine it directly.

Being so, the first step is to create a cycle 'for' which will go through all the elements and determine the connectivity of each element, to later obtain the coordinates of each vertex. Once determined the coordinates of the four vertices, it is possible to determine the coordinates of the center. It is not as straightforward given the fact that the elements are not always rectangles.

In order to determine the centroide, one diagonal should be drawn and the center of each triangle (represented in yellow) is determined, as exemplified in figure 4.

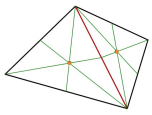

Figure 4: Step 1

The other diagonal is drawn and the centers of the two triangles (represented in green) are also determined (Figure 5).

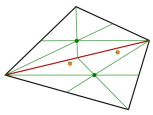

Figure 5: Step 2

Finally, the intersection point of the four points previously determined is the centroide of the quadrilateral.

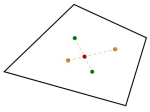

Figure 6: Step 3

Once the center is determined, it is finally possible to use equation 1, and determine the angle θ for each element.

3.2. Path Planning Algorithm

One of the variables to be optimized was the printing time, and in order to do so, it was necessary to define a path planning.

The main goal when implementing the algorithm was to obtain a robust and continuous deposition path planning, and without causing under-deposition or over-disposition. Raster filling pattern has been developed given the need of providing directional properties to printed composites.

This algorithm was based in [11], and it was implemented in MATLAB.

The design of the part is done using a CAD software, and then imported as an ASCII STL file to MATLAB.

Important information regarding each layer is required before the definition of the deposition points. There are outer curves enclosing the inner contour curves, and the minimum and maximum points are determined along the scanning direction.

Raster fill methodology is used to generate a continuous deposition path along the scanning direction. The algorithm is implemented to obtain printing instructions for complex geometries.

When printing a part, it is divided in several layers along the z direction, also known as the slicing process, and each layer is filled sequentially and independently.

Regarding the determination of the deposition path points are obtained by intersection of several lines along the y axis, within a distance of D between each line, with the outer contour. This distance is pre-defined, and in this case it will be considered 0.1mm (which is the layer resolution of the Markforged Mark Two Industrial Strength® 3D Printer). In order to reproduce the path planning in MATLAB, the equation used to plot the lines is:

$$y = tan(\alpha)x + b \tag{3}$$

where α is the angle of the fibers and b is the value of y when x=0.

There are 2 cases that must be considered regarding only convex shapes: the existence or not of holes.

In the simpler case without holes, each horizontal line produces two intersection points. The lines are referred as either "even" line or "odd" line, being the first line "even", the second "odd", and so on. Regarding the intersection points, in the even line, it goes from ip_0 to ip_1, and in the odd line it goes the other way round, from ip_1 to ip_0. A scheme is introduced in figure 7, in order to clarify what was explained in this paragraph.

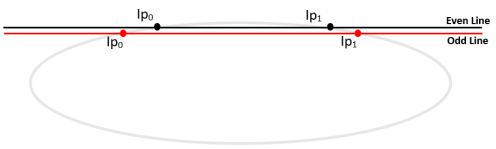

Figure 7: Raster Filling scheme

The part is created by filling from the layer with smallest z to the layer with the higher z. After filling one layer, the nozzle moves upwards, and the process carries on until the whole part is generated.

Considering the parts with holes, the process described until here cannot be applied since there is some information missing, such as the number of intersection points along each line.

This stage of the process is one of the most important, since it will be essential to avoid unfilled regions and deposition outside the part, two significant causes of loss of stiffness.

Lines are generated along the scanning direction spaced by D. However, the curved portions between two consecutive lines have to be considered and are divided into points with small increments. If the x coordinate of a point p_q is greater than p_{q-1} and p_{q+1}, then p_q can be approximated as a maximum point. In the same way, if p_q is smaller than p_{q-1} and p_{q+1}, then it is considered a minimum point.

In concave shapes, or when there are holes in the part, when moving from an even line to an odd line, the deposition points can be far from each other in terms of x, meaning that there is a possibility of a deposition outside the boundaries of the part occur.

To prevent it from happening, whenever the horizontal lines are intercepting the boundaries of the part more than three times, then, it is possible to define that between the second and the third point, along each line, there cannot be deposition.

In order to check if this is happening or not, it is taken the curve between two consecutive lowest x points. If the y value is increasing, then there is no deposition outside the curve. If the y values are decreasing, then there is deposition.

An example of path planning is introduced in the figure below for 30 degrees:

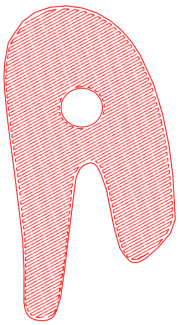

Figure 8: Path Planning for 30 degrees.

The path planning algorithm with fixed angle is easy to both design and manufacture. Besides, it fulfills the requirement of strength and technology. However, it fails to explore the performance of the fiber to its fullest.

In this process, the variable angle path planning algorithm is that the fiber laying angle is always changing during the process. This angle is defined as the intersection angle between the direction of the fibre laying and the x axis and which is always changing.

The path planning algorithm is exactly the same. However, instead of straight lines, curved lines are plotted using equation 2. The same example used for straight fibers will also be introduced (Figure 9), this time with curved fibers.

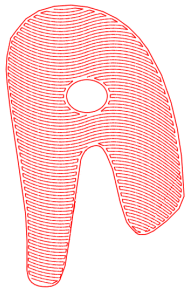

Figure 9: Path Planning for $T_0 = 0.45$, $T_1 = -0.35$ and $\phi = 0$.

Once the path planning is explained, it is also important to describe the computation of the printing time, since besides the continuous path planning, the main goal was to optimize the printing time.

In order to do so, it was first necessary to choose which printer to use. Previous in this work, it was mentioned that the Markforged Mark Two Industrial Strength® 3D Printer is the best in the market for CFRP composites and VAT composites, and it was used already in some researches and provided very good results [12].

However, not enough details of the printer are available, since for the model described in [13], it was mandatory to know the maximum and minimum velocities of the nozzle and the acceleration. In [13], the printer used is not specified, however, since the path planning strategy was the same and also the technique (FDM), the values used were assumed accurate for this work.

3.3. Printing Time

In zigzag path planning, it is possible to find two different types of lines *Type I* and *Type II*. The *Type I* zig zag lines form the main path whereas *Type II* zigzag lines are the connection lines between two *Type I* lines. An example is introduced next, in order to clarify the difference between the lines:

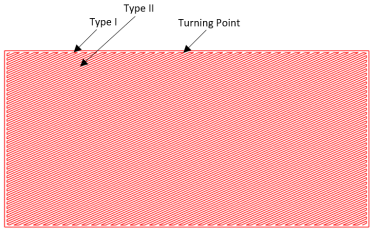

Figure 10: Types of zigzag lines

For both types of lines, the procedure when talking about the nozzle head is exactly the same: it starts with a minimum speed, afterwards it accelerates towards a maximum speed and then it decelerates to a minimum speed by the end it reaches the end of the line.

Having this said, the model aims to improve the efficiency of the process by accelerating or decelerating the

nozzle according to the geometrical characteristics. As thus, the following assumptions are made:

- The speed of the nozzle as from all the turning points in the minimum speed, V_{min};
- The maximum speed is represented as V_{max}. Both velocities vary according to the printer's settings, however, in this model the assumption is that V_{max} equals twice V_{min};
- The velocity of the nozzle along the zigzag path is either uniformly accelerated or decelerated, and the acceleration is represented by β.

The formulas for each type of line:

$$t(L_I) = \begin{cases} \dfrac{2V_{min}}{\beta}, & \text{if } L_I = \dfrac{3V_{min}^2}{\beta} \\ \dfrac{-2V_{min}}{\beta} + \sqrt{\left(\dfrac{2V_{min}}{\beta}\right)^2 + \dfrac{4L_I}{\beta}}, & \text{if } 0 < L_I < \dfrac{3V_{min}^2}{\beta} \\ \dfrac{2V_{min}}{\beta} + \dfrac{\beta L_I - 3V_{min}^2}{2\beta V_{min}}, & \text{if } L_I > \dfrac{3V_{min}^2}{\beta} \end{cases} \tag{4}$$

$$t(L_{II}) = \begin{cases} \dfrac{2V_{min}}{\beta}, & \text{if } L_{II} = \dfrac{3V_{min}^2}{\beta} \\ \dfrac{-2V_{min}}{\beta} + \sqrt{\left(\dfrac{2V_{min}}{\beta}\right)^2 + \dfrac{4L_{II}}{\beta}}, & \text{if } 0 < L_{II} < \dfrac{3V_{min}^2}{\beta} \\ \dfrac{2V_{min}}{\beta} + \dfrac{\beta L_{II} - 3V_{min}^2}{2\beta V_{min}}, & \text{if } L_{II} > \dfrac{3V_{min}^2}{\beta} \end{cases} \tag{5}$$

Even though the previous equations were only applied to 3D printing of straight fibers, they were also used for curved fibers. Further in this work, when the case studies are introduced, the values of both velocity and acceleration will be given. For simplicity, the same velocity was used for both types of fibers, even though in reality, the placement of VAT fibers is slower.

Besides this, what has changed when compared to straight fibers is the determination of the length of each curve, giving the fact that it is not as straightforward.

The formula implemented was the one that determines the length of a curve y=f(x) that goes from x=a to x=b:

$$L = \int_a^b \sqrt{1 + \left(\frac{dx}{dy}\right)^2} \tag{6}$$

3.4. Optimization

Most of the objective functions are formulated based on energy form, and strain energy formulation is one of the general formulation for optimization methods.

The objective function in this method aims to minimize the sum of all the element's strain energy. Using this concept of element strain energy, the deformations in all the directions are considered. Also, since strain energy and stiffness are inversely proportional, it means that a lower value of strain energy leads to a higher stiffness.

Strain Optimization The optimization problem is defined as [14]: finding the trade off between the best angle for the fibers, so that the stiffness of the work piece is maximized, and the minimum printing time. This stiffness is achieved in terms of strain energy of the work piece. The formulation of the optimization problem is:

$$\text{Minimize:} \qquad F = w_u \sum_{i=1}^{n} u_i + w_{time} \sum_{i=1}^{n} time_i \tag{7}$$

$$\text{Subject:} \qquad -90 < \alpha_i < 90 \tag{8}$$

where,
F: Objective function;
w_u: weight associated with the sum of the strain energy;
u: Strain Energy of Finite Elements;
w_{time}: weight associated with the printing time;
$time$: Printing time of the part;
n: Number of Elements.

Stress Optimization In this work, the function that is used is Kreisselmeier-Steinhauser (KS) [15]:

$$G_{ks} = \frac{1}{p} \ln \sum_{i=1}^{N} e^{p \dfrac{f_i(\sigma)}{f_{max}(\sigma)}} \tag{9}$$

where,
G: Objective function;
σ: Stress;
$f_{max}(\sigma)$: Maximum von Mises stress;
$f_i(\sigma)$: von Mises stress for each finite element;
$time$: Printing time of the part;
n: Number of Elements.

For this thesis in particular, it is also important to consider the printing time, as mentioned before, and being so, the ultimate objective function which have to be minimized is written as follows:

$$F = w_\sigma \frac{1}{p} \ln \sum_{i=1}^{N} e^{p \dfrac{f_i(\sigma)}{f_{max}(\sigma)}} + w_{time} \sum_{i=1}^{n} time_i \tag{10}$$

where,
F: Objective function;
w_σ: weight associated with the stress;
w_{time}: weight associated with the printing time;

The parameter p sets the difference between the original function and its approximation. A higher p means a more heavily weighted peak stress. However, it often leads to oscillation and divergence. The p considered is p=20 and its selection is beyond the scope of this thesis.

4. Results

4.1. Case Studies

The geometry of each case will be introduced at the same time the cases are described. The geometry, boundary

conditions and applied loads are the same for both straight and curved fibers.

However, before going further in detail in each one, considering the mechanical behaviour, further details have to be added to clearly define the theoretical framework of this work:

- The geometry of the laminate and the applied BCs are known and fixed;
- Each case, besides the 3D one, only considers one ply;
- The material behaviour is linear elastic;
- The VAT plate is quasi-homogeneous and fully orthotropic [16] [17] at each point of the structure.
- The speeds are assumed to be the same for both straight and curved fibers: $V_{max} = 20mm/s$, $V_{min} = 10mm/s$ and $\beta = 20mm/s^2$.

Furthermore, it is important to say that, in order for the results to be plotted, the distance between layers was increased, otherwise, if the 0.1mm between them were maintained, it would not be possible to understand the placement of the fibers.

The case studies are the following, for both straight and curved fibers:

- Shell Plate without hole;
- Shell Plate with hole;

The first case has 2 sets of boundary conditions (BC): Fully clamped with a constant pressure applied in the -z direction (Figure 4.1); Plate under traction (Figure 4.1). This case is introduced as a validation for the optimization process.

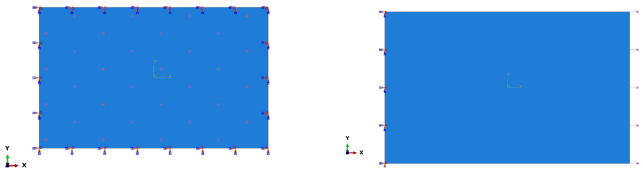

(a) Fully Clamped Plate under Uniform Pressure

(b) Plate under traction

Figure 11: Plate without a hole

The geometry of the shell plate with hole will only be analyzed under constant pressure, as represented in the Figure 12 below:

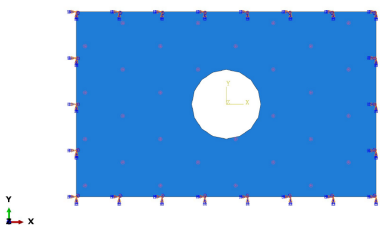

Figure 12: Fully Clamped Plate under uniform pressure

It is also important to clarify, how are the curved fibers defined in these geometries. Basically, the angle T_0 is defined in x=0, and the angle T_1 is defined in x=-13 and x=13, meaning that the length d is dependent on the angle phi, and finally, ϕ=0 it is aligned with the x axis. Furthermore, and as mentioned before, the curves following the first curve will be definied using a shifted method. Given this, and with the main goal of being able to define the curve along the whole length of the rectangle, then the angle ϕ will only vary between $-tg^{-1}(8/13)$ and $-tg^{-1}(8/13)$. The author is aware of the fact that this constraint will limit the results obtained, but the ones obtained will be significantly more accurate.

4.2. Shell Plate without hole

4.2.1 Strain Optimization

Straight Fibers Analyzing the table below, the results for when both weights were set to 0.5 and when the strain was given the weight of 1 are the same, fibers oriented to 90 degrees. When only the printing time was taken into account (i.e. $w_{time} = 1$), the best orientation is 0 degrees.

W_t	W_SE	PrintTime (s)	SE (J)
1	0	21270	5.689e+15
0.5	0.5	21520	1.461e+15
0	1	21520	1.461e+15

Table 2: Optimal solutions for the plate for different weight combinations - Strain Optimization

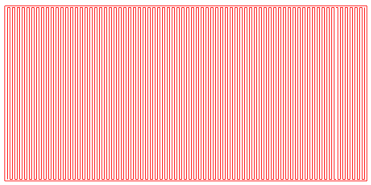

Figure 13: Strain Optimization for Straight fibers - Optimal Solution for the plate without a hole: $w_{time} = 0.5$ and $w_{strain} = 0.5$ & $w_{strain} = 1$ and $w_{time} = 0$

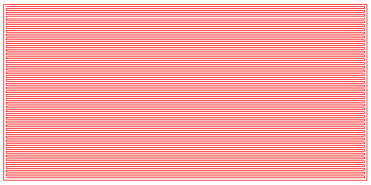

Figure 14: Strain Optimization for Straight fibers - Optimal Solution for the plate without a hole: $w_{strain} = 0$ and $w_{time} = 1$

Curved Fibers

Weight_t	Weight_SE	PrintTime (s)	SE (J)
1	0	22246	6.64e+15
0.5	0.5	47878	6.31e+15
0	1	43094	5.47e+15

Table 3: Optimal solutions for the plate for different weight combinations

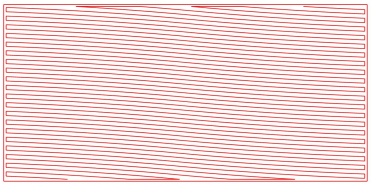

Figure 15: Strain Optimization for Straight fibers - Optimal Solution for the plate without a hole: $w_{strain} = 0$ and $w_{time} = 1$

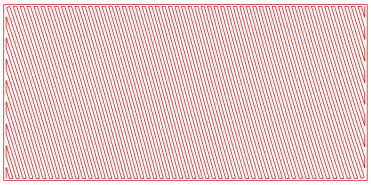

Figure 16: Strain Optimization for curved fibers - Optimal Solution for the plate without a hole: $w_{time} = 0.5$ and $w_{strain} = 0.5$

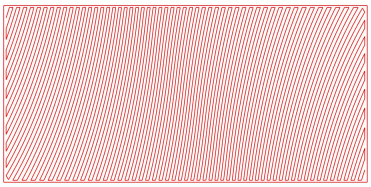

Figure 17: Strain Optimization for curved fibers - Optimal Solution for the plate without a hole: $w_{time} = 0$ and $w_{strain} = 1$

4.2.2 Stress Optimization

W_t	W_S	PrintTime (s)	Stress
1	0	21270	1.185
0.5	0.5	21520	1.256
0	1	21528	1.172

Table 4: Optimal solutions for the plate for different weight combinations - Stress Optimization

Curved Fibers

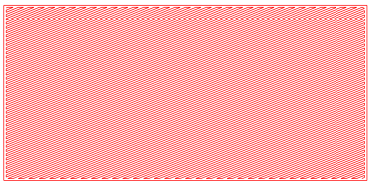

Figure 18: Stress Optimization for Straight fibers - Optimal Solution for the plate without a hole: $w_{time} = 0$ and $w_{strain} = 1$

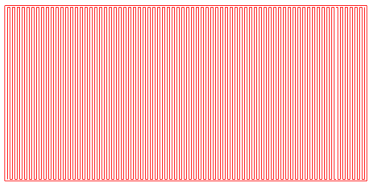

Figure 19: Stress Optimization for Straight fibers - Optimal Solution for the plate without a hole: $w_{time} = 0.5$ and $w_{strain} = 0.5$

Figure 20: Stress Optimization for Straight fibers - Optimal Solution for the plate without a hole: $w_{time} = 1$ and $w_{strain} = 0$

Weight_t	Weight_S	PrintTime (s)	Stress
1	0	22242	1.111
0.5	0.5	36688	1.138
0	1	47063	1.104

Table 5: Optimal solutions for the plate for different weight combinations

4.3. Shell Plate with a hole

4.3.1 Strain Optimization

W_t	W_SE	PrintTime (s)	SE (J)
1	0	20995	4.606e+15
0.5	0.5	20277	1.197e+15
0	1	20277	1.197e+15

Table 6: Optimal solutions for the plate with a hole for different weight combinations - Strain Optimization

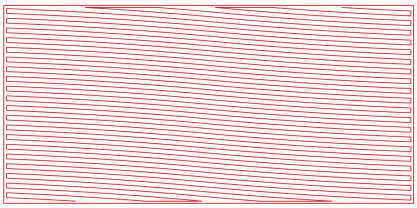

Figure 21: Stress Optimization for Curved fibers - Optimal Solution for the plate without a hole: $w_{time} = 1$ and $w_{stress} = 0$

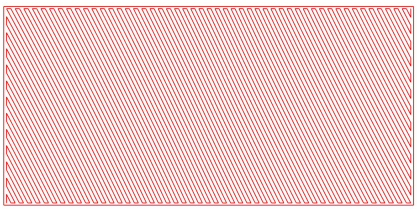

Figure 22: Stress Optimization for Curved fibers - Optimal Solution for the plate without a hole: $w_{time} = 0.5$ and $w_{stress} = 0.5$

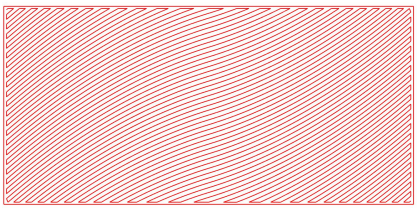

Figure 23: Stress Optimization for Curved fibers - Optimal Solution for the plate without a hole: $w_{time} = 0$ and $w_{stress} = 1$

Straight Fibers When both weights are set at 0.5, and when only strain energy is taken into account ($w_{strain} = 1$), the best orientation is 90 degrees, as represented in the following figure.

Weight_t	Weight_SE	PrintTime (s)	SE (J)
1	0	20983	4.64e+15
0.5	0.5	42752	2.05e+15
0	1	43831	1.78e+15

Table 7: Optimal solutions for the plate for different weight combinations

Curved Fibers

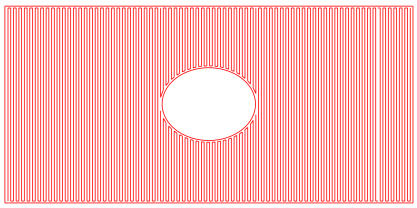

Figure 24: Stress Optimization for Straight fibers - Optimal Solution for the plate with hole: $w_{time} = 0.5$ and $w_{strain} = 0.5$ & $w_{strain} = 1$ and $w_{time} = 0$

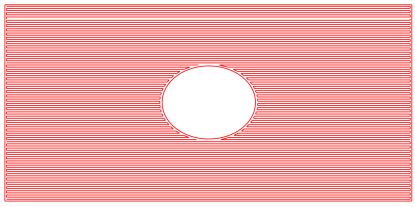

Figure 25: Stress Optimization for Straight fibers - Optimal Solution for the plate with hole: $w_{time} = 1$ and $w_{strain} = 0$

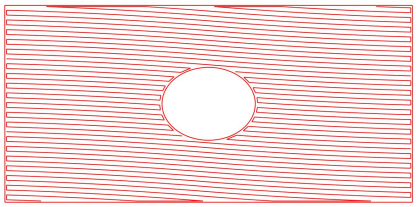

Figure 26: Strain Optimization for Curved fibers - Optimal Solution for the plate with hole: $w_{time} = 1$ and $w_{strain} = 0$.

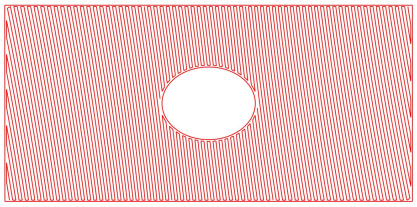

Figure 27: Strain Optimization for Curved fibers - Optimal Solution for the plate with hole: $w_{time} = 0.5$ and $w_{strain} = 0.5$.

4.3.2 Stress Optimization

Straight Fibers

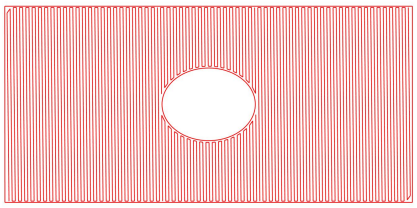

Figure 28: Strain Optimization for Curved fibers - Optimal Solution for the plate with hole: $w_{time} = 0$ and $w_{strain} = 1$.

Weight_t	Weight_S	PrintTime (s)	Stress
1	0	20995	1.143
0.5	0.5	21871	1.127
0	1	21871	1.127

Table 8: Optimal solutions for the plate with a hole for different weight combinations - Stress Optimization

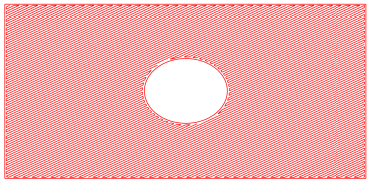

Figure 29: Stress Optimization for Straight fibers - Optimal Solution for the plate with a hole: $w_{time} = 0.5$ and $w_{strain} = 0.5$ & : $w_{time} = 0$ and $w_{strain} = 1$.

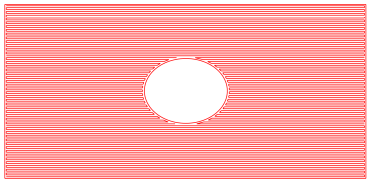

Figure 30: Stress Optimization for Straight fibers - Optimal Solution for the plate without a hole: $w_{time} = 1$ and $w_{strain} = 0$

Weight_t	Weight_S	PrintTime (s)	Stress
1	0	20983	1.158
0.5	0.5	23086	1.141
0	1	30030	1.091

Table 9: Optimal solutions for the plate for different weight combinations

Curved Fibers

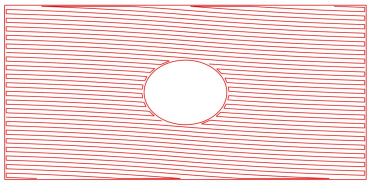

Figure 31: Stress Optimization for Curved fibers - Optimal Solution for the plate with a hole: $w_{time} = 1$ and $w_{stress} = 0$

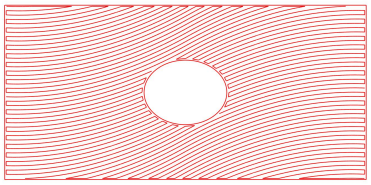

Figure 32: Stress Optimization for Curved fibers - Optimal Solution for the plate with a hole: $w_{time} = 0.5$ and $w_{stress} = 0.5$

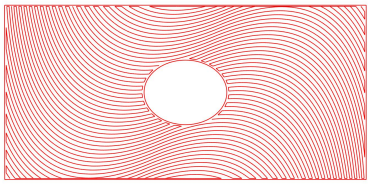

Figure 33: Stress Optimization for Curved fibers - Optimal Solution for the plate with a hole: $w_{time} = 0$ and $w_{stress} = 1$

5. Conclusions

5.1. Achievements

The thesis research aimed at providing an optimization tool for CFRP composites to maximize the structural performance and minimizing printing time. For that end, a path plannning algorithm was successfully implemented in MATLAB, for both curved and straight fibers. Both optimizations were implemented for different case studies, and different and coherent results were obtained.

5.2. Conclusions

An optimization framework has been developed for 3D printers to integrate the structural and the manufacturing perspectives.

Firstly, the path planning algorithm was successfully implemented in order to determine the printing time of the different parts. Even though not a lot of information is available regarding this matter, some values present in the literature were used, and adapted for the printing of the curved fibers model. Furthermore, this path planning and the computation of the printing time is adaptable to

every printer, as long as the information regarding the maximum and minimum velocity, the acceleration and the nozzle diameter is provided.

Regarding the optimization, first, a framework of structural optimization was developed where the printing time was integrated. Second, the framework itself is also easily adaptable to other printers and also to other objective functions. Moreover, and focusing now in the results, when only the time is considered, all the 2D models presented similar results. This is the first proof that the optimizer was working correctly. Since the geometries were very similar it would not make sense to have differences in the final design. Still considering the time, it has to be taken into account that only 1 ply is considered in this study. When the full model, with several plies, is contemplated, then the time difference is considerable. In addition, when the geometry with a hole is considered, it is possible to observe the adaptation of the curves around the hole, where the stresses are concentrated. This is another evidence of the success of the implementation of this framework.

Regarding the 3D specimen, this case study was not explored to its fullest, largely due to the amount of time needed to run the simulations, but also because it was not a priority goal of this work. However, it was also possible to observe curved adapting around the hole. For this case, it would also make sense to increase the number of design variables, in order to increase the freedom of design.

5.3. Future Work

Even though some interesting results were achieved, a lot of research still needs to be done in this field, in order to determine the best designs and the properties of the CFRP composites manufactured using AM.

Regarding the work presented, the next steps are the completion of the analysis of the 3D specimen, with a larger number of design variables.

Furthermore, the implementation of the path planning in a 3D printer in order to produce parts and to perform an experimental analysis, so that the results could be confirmed.

Another suggestion for further work in the matter is to consider different objective functions. In this work, besides strain and stress optimization, the printing time was also optimized. However, other parameters, equal or more important, could also be considered, such as: material cost and printing restrictions. The latter is particularly interesting and important, since the manufacturing process of VAT composites is highly complex.

A final suggestion for future work is to perform optimizations in more complex geometries.

References

[1] Carter WT, Erno DJ, Abbott DH, Bruck CE, Wilson GH, Wolfe JB, Finkhousen DM, Tepper A, Stevens RG. The GE aircraft engine bracket challenge: an experiment in crowdsourcing for mechanical design concepts. In25th Annual International Solid Freeform Fabrication Symposium, Austin, TX, Aug 2014 (pp. 4-6).

[2] Ning F, Cong W, Wei J, Wang S, Zhang M. Additive manufacturing of CFRP composites using fused deposition modeling: effects of carbon fiber content and length. InASME 2015 International Manufacturing Science and Engineering Conference 2015 Jun 8. American Society of Mechanical Engineers Digital Collection.

[3] Nebelsick JH, Allgaier C, Felbrich B, Coupek D, Reiter R, Reiter G, Menges A, Lechler A, Wurst KH. Continuous Fused Deposition Modelling of Architectural Envelopes Based on the Shell Formation of Molluscs: A Research Review. InBiomimetic Research for Architecture and Building Construction 2016 (pp. 243-260). Springer, Cham.

[4] Todoroki A, Watanabe K, Kobayashi H. Application of genetic algorithms to stiffness optimization of laminated composite plates with stress-concentrated open holes. JSME Int J 1995;38(4):458–64.

[5] Adams DB, Watson LT, Gurdal Z, Anderson-Cook CM. Genetic algorithm optimization and blending of composite laminates by locally reducing laminate thickness. Adv Eng Soft 2004;35:35–43.

[6] Puri G. Python scripts for Abaqus: learn by example. Gautam Puri; 2011.

[7] Kang JH, Kim CG. Minimum weight design of compressively loaded composite plates and stiffened panels for post-buckling strength by genetic algorithm. Compos Struct 2005;69:239–46.

[8] https://markforged.com/mark-two/ Retrieved August 28, 2019

[9] Melenka GW, Cheung BK, Schofield JS, Dawson MR, Carey JP. Evaluation and prediction of the tensile properties of continuous fiber-reinforced 3D printed structures. Composite Structures. 2016 Oct 1;153:866-75.

[10] Sauer MJ. Evaluation of the mechanical properties of 3D printed carbon fiber composites (Doctoral dissertation, Mechanical Engineering Department, South Dakota State University).

[11] Asif S. Modelling and path planning for additive manufacturing of continuous fiber composites (Doctoral dissertation).

[12] Catapano A, Montemurro M, Balcou JA, Panettieri E. Rapid Prototyping of Variable Angle-Tow Composites. Aerotecnica Missili Spazio. 2019 Dec 1;98(4):257-71.

[13] Jin GQ, Li WD, Gao L, Popplewell K. A hybrid and adaptive tool-path generation approach of rapid prototyping and manufacturing for biomedical models. Computers in industry. 2013 Apr 1;64(3):336-49.

[14] Ahmad Z, Zoppi M, Molfino R. Fixture Layout Optimization Using Element Strain Energy and Genetic Algorithm. World Academy of Science, Engineering and Technology, International Journal of Mechanical, Aerospace, Industrial, Mechatronic and Manufacturing Engineering. 2013 Sep 1;7(10):1924-30.

[15] Yang RJ, Chen CJ. Stress-based topology optimization. Structural optimization. 1996 Oct 1;12(2-3):98-105.

[16] Catapano A, Montemurro M. A multi-scale approach for the optimum design of sandwich plates with honeycomb core. Part II: the optimisation strategy. Composite structures. 2014 Dec 1;118:677-90.

[17] Montemurro M, Catapano A, Doroszewski D. A multi-scale approach for the simultaneous shape and material optimisation of sandwich panels with cellular core. Composites Part B: Engineering. 2016 Apr 15;91:458-72.

[18] Norman DA, Robertson RE. The effect of fiber orientation on the toughening of short fiber-reinforced polymers. Journal of applied polymer science. 2003 Dec 5;90(10):2740-51.

[19] Naresh K, Krishnapillai S, Velmurugan R. Effect of fiber orientation on carbon/epoxy and glass/epoxy composites subjected to shear and bending. InSolid State Phenomena 2017 (Vol. 267, pp. 103-108). Trans Tech Publications.